Research Journal of Applied Sciences, Engineering and Technology 8(18): 1953-1965, 2014
DOI:10.19026/rjaset.8.1187
ISSN: 2040-7459; e-ISSN: 2040-7467

Submitted: July 14, 2014 Accepted: August 26, 2014 Published: November 15, 2014

**Research Article**

# Numerical Study of a Solar Chimney Power Plant

[1]A. Dhahri, [1]A. Omri and [2]J. Orfi
[1]Department of Materials, Energy and Renewable Energies, College of Sciences, University of Gafsa, 2112 Gafsa, Tunisia
[2]Department of Mechanical Engineering, King Saud University, P.O. Box 800, Riyadh, 11421, KSA

**Abstract:** The aim of this study is to present a numerical analysis on the performance of a solar chimney power plant using steady state Navier-Stokes and energy equations in cylindrical coordinate system. The fluid flow inside the chimney is assumed to be turbulent and simulated with the k-ε turbulent model, using the FLUENT software package. Numerical simulations were performed using the Spanish prototype as reference. The computed results are in good agreement with experimental measurements of Manzanares power plant. Besides, a theoretical model was proposed taking into account the kinetic energy difference within the solar collector. The effects of the main geometrical parameters of the collector and the solar radiation intensity on the air mass flow rate and the temperature rise in the collector have been investigated. The fluid and ground temperature distributions were also presented and analyzed.

**Keywords:** Numerical simulation, renewable energy, solar chimney, solar energy

## INTRODUCTION

Due to current concerns about global warming, fossil resources depletion and the increase in global energy and electric needs, energy technologies based on renewable sources have seen rapid change in recent years. There is an immediate potential for the exploration and use of renewable energy sources such as wind, solar and geothermal energy in various applications including power generation and desalination. Several countries have encouraged the development of reliable and simple hybrid installations for arid and semi-arid areas. These conditions are suitable to the development of solar power generation technologies (Huang *et al*., 2007; Schlaich, 1995). The solar chimney power plant which is an example of such technologies was first proposed by professor Jörg Schlaich and tested with a prototype model in Manzanares, Spain in the early 1980s (Lorente *et al*., 2010). This power plant operated for approximately eight years generating 50 kW output. Haaf *et al*. (1983) discussed the basic principles, energy balance, construction and cost analysis of a solar chimney power plant. Later, they presented preliminary results from the Spanish prototype (Haaf, 1984). In the first part of their work, Pasumarthi and Sherif (1998a) developed a mathematical model to predict temperature and power production and to study the effect of several ambient conditions and geometric dimensions on power output. In the second part, they carried out theoretical and experimental studies on the solar chimney plant performance. The target of this study was to demonstrate the viability of the plant as a power generating system. Besides, Pasumarthi and Sherif (1998b) have tested three different configurations of the solar collector.

Due to the high construction cost of a large scale solar chimney power generating systems, numerical studies have been carried out by many researchers using the solar chimney prototype in Manzanares as a reference. Pastohr *et al*. (2004) carried out an analysis to improve the description of the operation mode and efficiency of solar chimney power plant. Authors modeled all system parts (collector, chimney, turbine and ground) numerically based on the Manzanares prototype geometric parameters. Fluent software was used to handle the numerical solution. Bernardes *et al*. (1999) conducted a numerical simulation of laminar natural convection in a solar tower. For the prediction of thermo-hydrodynamic behavior of the system, the numerical model was developed using the finite volume method in generalized coordinates. Ming *et al*. (2006) analyzed the influence of various parameters (solar radiation, collector radius and chimney height) on the relative static pressure, driving force, power output and the system efficiency. Later, the same team (Ming *et al*., 2008a) performed numerical simulations to investigate the characteristics of flow and heat transfer system which includes a layer of energy storage.

**Corresponding Author:** J. Orfi, Department of Mechanical Engineering, King Saud University, P.O. Box 800, Riyadh, 11421, KSA

Mathematical models of the collector, the chimney and effects of different solar radiation on the characteristic of heat storage layer were analyzed. Ming *et al*. (2008b) conducted a numerical study of a solar chimney coupled with a 3-blade turbine. They have presented the effect of turbine rotational speed on the power plant outlet parameters. To give a reference to the design of large scale solar chimney, authors have performed a numerical simulation of a MW-grade solar chimney. Huang *et al*. (2007) have used the Spanish prototype as a model to study the effect of solar radiation on various parameters such as upwind velocity, temperature difference between the inlet and outlet of collector and the differential pressure of the collector-chimney transition section. Fluent software was used to obtain the numerical solution. More recently, Ming *et al*. (2010) performed a study of the fluid flow inside many parts of the solar chimney and established an analysis of the thermodynamic cycle. Zheng *et al*. (2010) have developed a mathematical model to analyze heat and mass transfer in a solar chimney power plant with an energy storage layer. Based on an unsteady numerical simulation, they have studied the effect of some energy storage materials under different solar radiation on the system power output. Chergui *et al*. (2010) modeled numerically the process of laminar natural convection in a solar chimney. They have focused on airflow and heat transfer inside the system and analyzed the effect of the geometry and Rayleigh number. The numerical solution was obtained using the formulation in primitive variables (velocity-pressure) with the finite volume method. Sangi *et al*. (2011) conducted a numerical analysis of a steady state two dimensional axisymetric model of a solar chimney system. The obtained results were compared fairly with the experimental data of the Spanish prototype. Besides the storage medium have been established and the Xu *et al*. (2011) performed numerical simulations on air flow, heat transfer and power output characteristics of a solar chimney power plant model with energy storage layer and turbine using the Spanish prototype characteristics.

The aim of this study is to propose theoretical models to analyze the performance of solar chimney power plant under various conditions of solar radiation and geometrical dimensions. First, a simplified global model is proposed. A numerical model is also developed and the results from a parametric study are presented and analyzed.

## SYSTEM DESCRIPTION

The solar chimney is a way to produce electric power from solar radiation. It is a device combining three known technologies including: a huge greenhouse called “collector”, a chimney placed in the center of it and one or more turbines connected to generators. The solar chimney is based on the idea of using the natural convection of air heated by the sun rays. The collector covered by glass or transparent plastic roof, guides the heated air. This hot air, naturally aspirated through the chimney, is continuously renewed by the air on the outskirts of the greenhouse. The kinetic energy of air is then drawn through a system of turbines and generators which convert this fraction of energy into mechanical energy then into electrical energy. The main advantage of this system is that it can operate without using intermittent radiation from the sun during the day and the heat stored in the soil at night (Fig. 1).

In this study, the main dimensions of the physical model shown in Fig. 1 were selected according to the

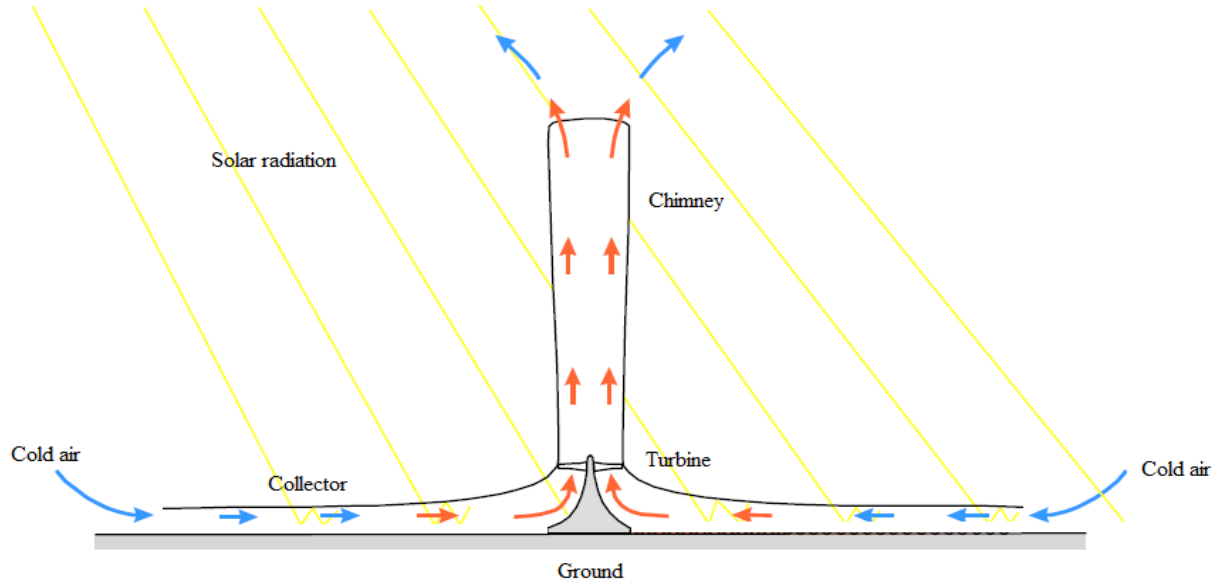


Fig. 1: Solar chimney power plant description

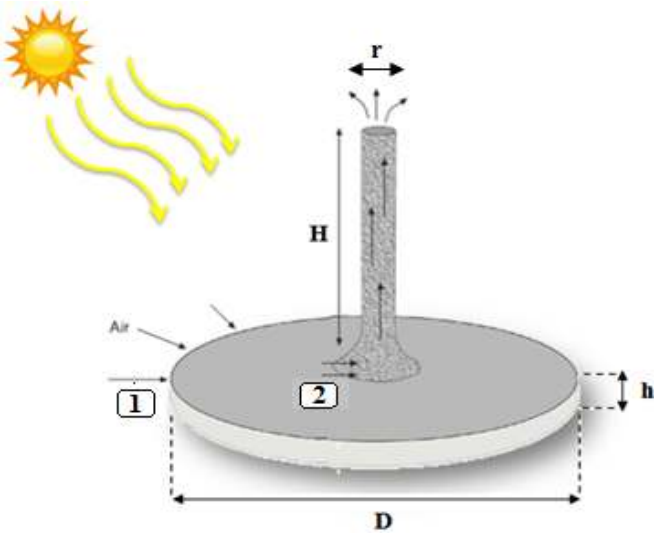


Fig. 2: Solar chimney power plant computational domain

Spanish prototype. The system geometry consists of a chimney with 200 m height and 5 m radius surrounded by a collector with 120 m radius and 1.85 m height. The chimney and the collector are separated by a transition section where a turbine driven by the updraft is placed. The solar chimney configuration has the four dimensions shown in Fig. 2: D, H, r and h.

## MATHEMATICAL MODELS

In this study, a mathematical model of solar chimney power plant has been developed to analyze heat transfer of air inside the system. To formulate this model the following assumptions were made:

- The fluid is Newtonian and in compressible.
- The flow is stationary, three-dimensional and turbulent.
- The axsymmetric flow is assumed.
- The viscous dissipation and compressibility effects are assumed negligible.
- The Boussinesq approximation is assumed to be valid. According to this approximation all variation of properties are assumed constant except for density in the momentum equation.

The description of fluid motion is carried through the conservation equations of mass, momentum and energy. Closure for the unknowns in the above equations can be obtained by the application of suitable turbulence models. The k-ε models are used as closure equations and standards values for constants are adopted.

With the assumptions expressed above and in the case of a steady state, basic equations can be written in cylindrical coordinates as follows.

**Continuity equation:**

$$\frac{1}{r}\frac{\partial}{\partial r}(ru)+\frac{\partial w}{\partial z}=0 \tag{1}$$

**Momentum equations:**

$$\rho\left(u\frac{\partial u}{\partial r}-\frac{v^2}{r}+w\frac{\partial u}{\partial z}\right)=-\frac{\partial p}{\partial r}+\mu\left[\frac{1}{r}\frac{\partial}{\partial r}\left(r\frac{\partial u}{\partial r}\right)-\frac{u}{r^2}+\frac{\partial^2 u}{\partial z^2}\right] \tag{2}$$

$$\rho\left(u\frac{\partial v}{\partial r}+\frac{uv}{r}+w\frac{\partial v}{\partial z}\right)=\mu\left[\frac{1}{r}\frac{\partial}{\partial r}\left(r\frac{\partial v}{\partial r}\right)-\frac{v}{r^2}+\frac{\partial^2 v}{\partial z^2}\right] \tag{3}$$

$$\rho\left(u\frac{\partial w}{\partial r}+w\frac{\partial w}{\partial z}\right)=-\frac{\partial p}{\partial z}+\rho g\beta(T-T_c)+\mu\left[\frac{1}{r}\frac{\partial}{\partial r}\left(r\frac{\partial w}{\partial r}\right)+\frac{\partial^2 w}{\partial z^2}\right] \tag{4}$$

**Energy equation:**

$$\frac{1}{r}\frac{\partial}{\partial r}(\rho ruT)+\frac{\partial}{\partial z}(\rho vT)=\frac{1}{r}\frac{\partial}{\partial r}(r\frac{\lambda}{c_p}\frac{\partial T}{\partial r})+\frac{\partial}{\partial z}(\frac{\lambda}{c_p}\frac{\partial T}{\partial z}) \tag{5}$$

**k and ε equations:**

$$\rho\left(\frac{1}{r}\frac{\partial(ruk)}{\partial r}+\frac{\partial(kv)}{\partial z}\right)=\frac{\partial}{\partial z}\left(\left(\mu+\frac{\mu_t}{\sigma_k}\right)\frac{\partial k}{\partial z}\right)+\frac{1}{r}\frac{\partial}{\partial r}\left(r\left(\mu+\frac{\mu_t}{\sigma_k}\right)\frac{\partial k}{\partial r}\right)+G_k-\rho\varepsilon \tag{6}$$

$$\rho\left(\frac{1}{r}\frac{\partial(ru\varepsilon)}{\partial r}+\frac{\partial(\varepsilon v)}{\partial z}\right)=\frac{\partial}{\partial z}\left(\left(\mu+\frac{\mu_t}{\sigma_\varepsilon}\right)\frac{\partial \varepsilon}{\partial z}\right)+\frac{1}{r}\frac{\partial}{\partial r}\left(r\left(\mu+\frac{\mu_t}{\sigma_\varepsilon}\right)\frac{\partial \varepsilon}{\partial r}\right)+\frac{\varepsilon}{k}(c_1G_k-c_2\rho\varepsilon) \tag{7}$$

In the equations above, $G_k$ represents the generation of turbulence kinetic energy due to the mean velocity gradients. For the standard k-ε model, the constants have the following values (Zheng *et al*., 2010):

$C_1 = 1.44$, $C_2 = 1.92$, $\sigma_k = 1.0$, $\sigma_\varepsilon = 1.3$

**Heat balance of the collector:** The collector is a key device in the solar chimney power plant. It is capable to convert solar energy into thermal energy which be later converted into kinetic and electric energy. Some studies found in the literature (Schlaich, 1995; Dai *et al*., 2003; Schlaich *et al*., 2005) considered the theoretical basic collector model (model 1) proposed by Schleicher to analyze the mechanism of heat transfer in the collector. For simplicity and minimization of calculation efforts, this model ignored the role of the kinetic energy difference inside the collector and supposed that its contribution can be neglected. The researchers recommended that the energy equation balance is given as:

$$\dot{Q} = \dot{m} Cp \Delta T = (\tau\alpha) A_{coll} G - h_{conv} \Delta T_a A_{coll} \quad (8)$$

where,

$G$ = Solar radiation
$A_{coll}$ = Collector area
$\dot{Q}$ = Heat output of warm air
$Cp$ = Specific heat capacity of air
$\dot{m}$ = The mass flow rate of air flowing through the solar collector and which is expressed by:

$$\dot{m} = \rho_{coll} A_2 V_2 \quad (9)$$

Substituting (9) in (8), the velocity at the exit of the collector can be given by:

$$V_2 = \frac{(\tau\alpha) A_{coll} G - h_{conv} \Delta T_a A_{coll}}{\rho_{coll} A_c Cp \Delta T} \quad (10)$$

In this study, we adjusted the energy equation balance in the collector (model 2) by taking into account the kinetic energy contribution. In this case the following equation shall be used:

$$\frac{G}{\rho_{coll} A_2} + \frac{\phi_p}{\rho_{coll} A_2} + \frac{A_1}{A_2}\left(C_p V_1 T_1 + \frac{V_1^3}{2}\right) = C_p V_2 T_2 + \frac{V_2^3}{2} \quad (11)$$

The heat flow lost by convection between the collector and the environment is given by:

$$\phi_p = -h_{conv} A_{coll} (T_c - T_{air}) \quad (12)$$

where, $A_1$, $A_2$ et $A_{coll}$ are expressed respectively by:

$$A_1 = 2\pi R h_{coll} \ , \ A_2 = 2\pi r h_{coll} \text{ and } A_{coll} = \pi R^2$$

Thereby, the air collector exit velocity can be obtained as follows:

$$V_2 = \sqrt[3]{-\frac{q}{2} - \frac{1}{2}\sqrt{\frac{27q^2 + 4p^3}{27}}} + \sqrt[3]{-\frac{q}{2} + \frac{1}{2}\sqrt{\frac{27q^2 + 4p^3}{27}}} \quad (13)$$

where,

$$p = 2C_p T_2 \quad (14)$$

$$q = -\frac{2G}{\rho_{coll} A_2} + \frac{2h_{conv} A_{coll} (T_c - T_{air})}{\rho_{coll} A_2} - 2V_1 \frac{A_1}{A_2}\left(C_p T_1 + \frac{V_1^2}{2}\right) \quad (15)$$

## CFD MODELING

Due to the complexity and high cost of experimental measurement techniques, CFD has seen significant growth over the last decades. It has been widely applied to various engineering applications. In this study, results are calculated with the commercial FLUENT software (Fluent Inc., 2005). The geometry and configurations considered in this study correspond to those of the Spanish model.

**Geometry construction and grid generation:** To better control the construction of the mesh, we divided the computational domain into several zones (sub-volumes). There are three different parts i.e., the collector, the transition section and the chimney. The mesh of each part was generated separately. The transition zone is the most sensitive area of the computational domain as it is a very small area on which there is a strong pressure gradient (Schlaich, 1995). This requires a very fine mesh in this area by adopting the tetrahedral mesh. The other two sub-volumes are meshed using hexahedral mesh (Fig. 3).

**Boundary conditions:** An inlet pressure boundary condition type is specified at the collector inlet. Pressure outlet boundary condition type is specified at the chimney outlet. For both inlet and outlet of the system a standard atmospheric pressure condition was prescribed. In FLUENT, the gauge pressure boundaries are fixed to 0 Pa. It can be explained by the fact that the inlet collector and the exit chimney pressures are equal to the atmospheric value at the same altitude (Pastohr *et al*., 2004). The ambient temperature in the calculations is 293 K. Non-slip conditions are imposed

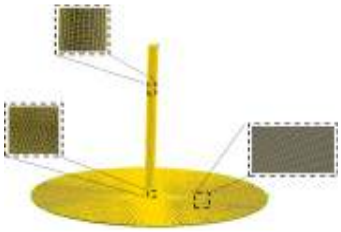

Fig. 3: Numerical grid

on the walls. The ground surface boundary condition is modeled as a no-slip wall with constant heat flux. The amount of heat flux from the ground surface is 640 W/m$^2$ (the absorptance of the soil is 0.8). The chimney walls are considered to be adiabatic. The details of boundary conditions are shown in Table 1.

**Numerical procedure:** As mentioned above, the conservation equations are solved numerically with FLUENT code using a steady state 3D implicit solver. Pressure-velocity coupling was accomplished by means of the SIMPLE algorithm (Patankar, 1980; Versteeg and Malalasekera, 2007). Initially the first order upwind scheme was used to get an approximate solution. Then the model was solved with a standard second order upwind discretization scheme using the default under-relaxation constants. Pressure interpolation was done using the PRESTO method (Versteeg and Malalasekera, 2007). At the entrance of the collector, the inlet temperature is considered equal to the ambient temperature.

A convergence criterion of $10^{-3}$ was imposed on the residuals of the continuity equation, momentum equation and velocity components. For the solution of energy equation a convergence criterion of $10^{-6}$ was chosen. In order to check the grid independence of solution, a series of calculations were carried out for several grid sizes. Four mesh configurations were tested in this study to determine the best compromise between accuracy of From the grid in independence results and computation time. tests, it was found that the grid with 1228452 cells is appropriate for the present application.

## RESULTS AND DISCUSSION

**Validation model:** In order to validate the developed model, the numerical results are compared with experimental and numerical data available in the literature. Firstly, the CFD results are compared with the experimental data of the Spanish plant of Manzanares (Haaf *et al*., 1983). The computational domain was simulated for two different values of solar radiation (800 and 1000 W/m$^2$), maintaining the other parameters of the system fixed. Table 2 shows that simulation results are quite consistent with experimental measurements of the Spanish prototype.

The second comparison was made with numerical results given by Huang *et al*. (2007). In this study, Huang *et al*. (2007) considered a three dimensional case of a solar chimney with the same geometric parameters and under the same weather conditions of Manzanares power plant. The static pressure in the chimney, the velocity at the entrance of the chimney and the temperature difference between inlet and outlet of the collector are computed numerically and compared with the results of Huang *et al*. (2007). Figure 4 illustrates the pressure distribution at different heights of the chimney. The calculated and reference pressures in the chimney are compared and the agreements are good except in the area near the entrance of the chimney where slight deviations are observed. It is shown from Fig. 4 that the pressure increases gradually as the air is flowing inside the chimney. It indicates also that the minimum static pressure is reached near the chimney base.

Figure 5 illustrates the air velocity distribution inside the transition section as function of the solar radiation intensity ranging from 100 to 900 W/m$^2$. Figure 5 show that when geometrical dimensions of the system are constant, raising the solar radiation intensity increases the air velocity. The increase is significant for low values of solar radiation intensity. The comparison between the profiles predicted in the present study and

Table 1: Settings of the main boundary conditions (Huang *et al*., 2007)

| Position | Type | Value |
|---|---|---|
| Collector inlet | Pressure inlet | $T_0$ = 293 K, $\Delta P$ = 0 Pa |
| Chimney outlet | Pressure outlet | $\Delta P$ = 0 Pa |
| Transparent covering | Convection heat transfer | $h_{conv}$ = 8 W/m$^2$.K, |
| Soil | Constant heat source | Q = $I_0$ ($\alpha$), W/m$^2$ |
| Chimney wall | Adiabatic wall | 0 W/m$^2$ |

Table 2: Comparison between numerical and experimental results

| Solar radiation (W/m$^2$) | | This model | Experimental data (Haaf *et al*., 1983) |
|---|---|---|---|
| 800 | Upwind velocity (m/sec) | 12.3273 | 12 |
| | $\Delta$T (°C) | 17.7830 | 17 |
| 1000 | Upwind velocity (m/sec) | 14.0060 | 15 |
| | $\Delta$T (°C) | 19.2770 | 20 |

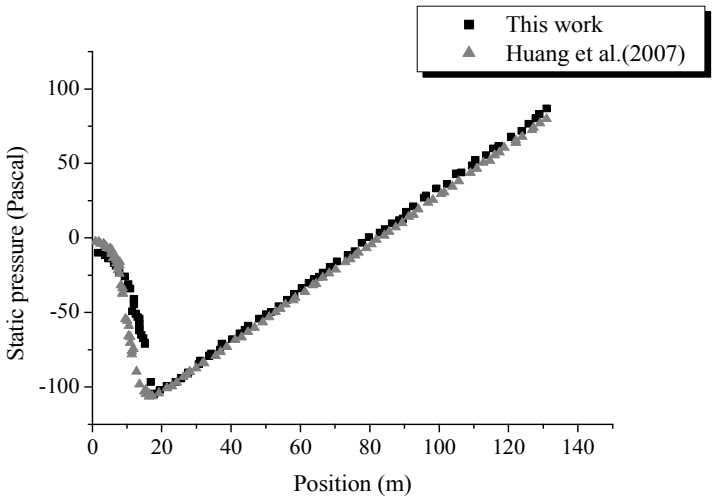


Fig. 4: Pressure distribution inside the chimney

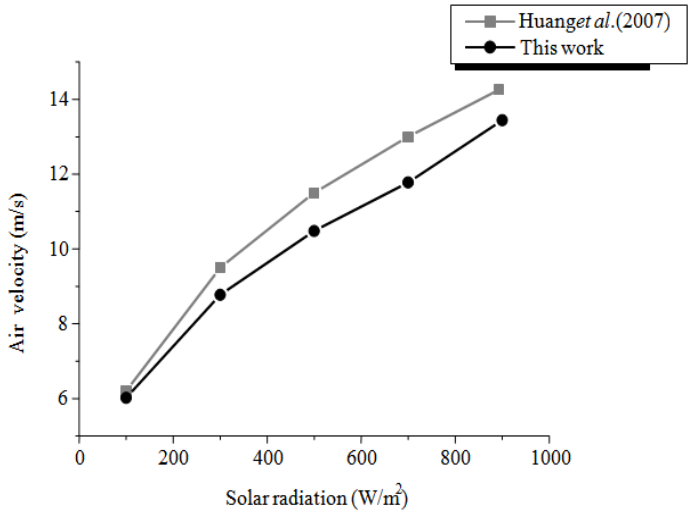


Fig. 5: Effect of solar radiation on air velocity at the collector outlet

those given by Huang *et al*. (2007), shows a fairly good agreement with an average difference of about 7%. Such differences between the results of the two models may be attributed to several reasons including the different assumptions and correlations for the evaluation of fluid properties used in both studies.

A third comparison was also performed between the numerical results of Huang *et al*. (2007) and the current CFD predictions. Figure 6 compares the increase in temperature (defined as the difference between the inlet and outlet Temperature ($\Delta T$)) distribution along the collector in terms of solar radiation. It shows an almost linear behavior relating the increase in fluid temperature and the solar radiation. The agreement between the computed results and those of Huang *et al*. (2007) is very good.

Based on the above tests of validation, the reliability of the computer code is confirmed. Therefore, the developed numerical model can be used to investigate the problem of flow with heat transfer inside a solar chimney system.

In the following, the kinetic energy contribution is first discussed using two separate analytical models and the CFD model. Then, a parametric study using the numerical model is conducted to investigate the effect of the collector radius, collector entrance height, chimney height on the performance of solar power plant.

**Kinetic energy contribution:** In order to analyze the influence of the kinetic energy contribution inside the collector, we proposed to study the models presented in section mathematical models. For this purpose, we have developed two iterative programs. The Spanish prototype operating conditions were considered as inputs. According to Eq. (10) and (13), we can conclude that the air exit velocity is a function of the collector size and the solar radiation intensity. Taking a constant

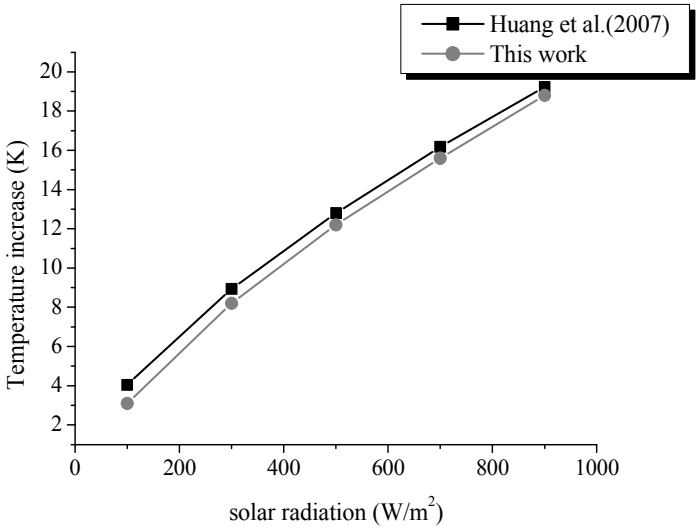


Fig. 6: Effect of solar radiation on temperature increase in the collector

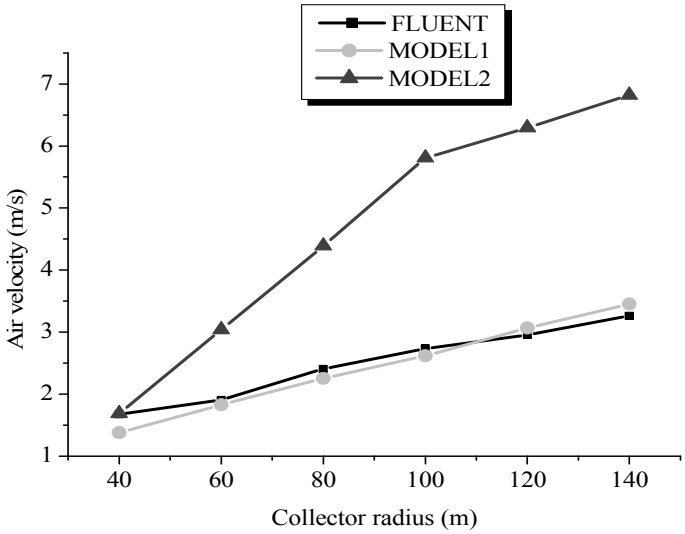


Fig. 7: Effect of collector radius on air exit velocity using CFD and models 1 and 2 (solar intensity = 800 W/m$^2$)

solar radiation of 800 W/m$^2$, the air velocity distribution is obtained using Eq. (10) and (13) as well as CFD code. Six different values of the collector radius (40, 60, 80, 100, 120 and 140 m, respectively) are used. The results are depicted in Fig. 7. This Figure shows a very good agreement between the second model (model 2) and numerical results. It can be seen that the collector radius has a significant influence on the velocity distribution. The comparison of the profiles as calculated using the reference model (model 1) and the current model (model 2), demonstrates that Schlaich model overestimates the values of the air velocity. Significant differences between the two profiles can be seen. These differences can have an average value of about 18% for a collector radius of 40 m while it reaches 51% when the collector radius is equal to 120 m.

For the second analysis the collector radius was maintained constant at 120 m. Figure 8 shows the effect of solar radiation on the collector exit velocity using the two analytical models (1 and 2). It can be easily seen from this figure that the collector exit velocity is only 1.91 m/sec when the kinetic energy change term is added to the energy balance equation, while the velocity reaches 3.55 m/sec when it is neglected. From Fig. 7 and 8, it is found that the kinetic energy contribution has a significant effect on the air velocity at the collector exit and must be included in the energy balance on the collector.

**Parametric study:** The numerical model is used to perform a parametric study on the effect of the collector dimensions and solar radiation intensity on the main

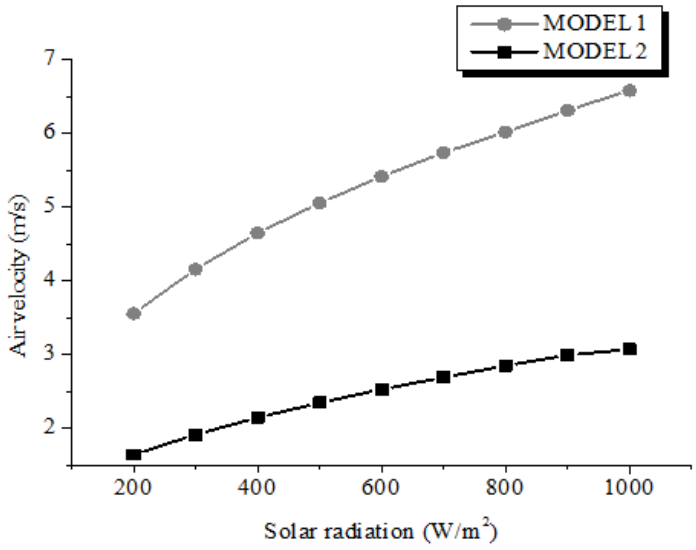


Fig. 8: Effect of solar radiation on air exit velocity using models 1 and 2 (collector radius = 120 m)

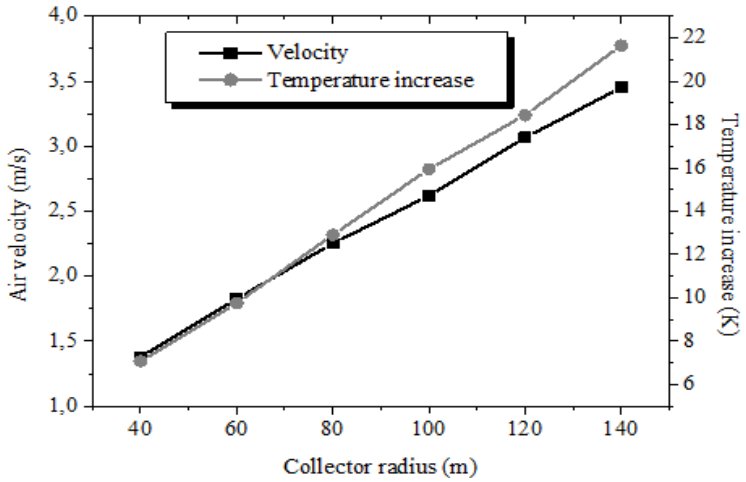


Fig. 9: Temperature rise and velocity distribution versus collector radius (solar radiation = 800 W/m$^2$)

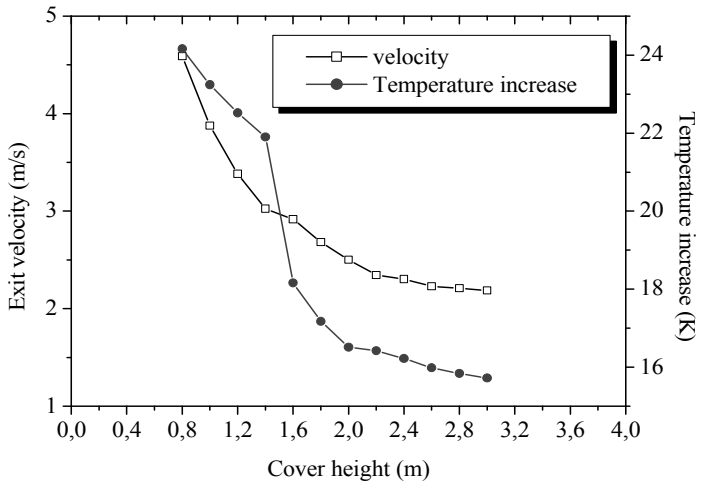


Fig. 10: Temperature rise and velocity distribution with cover height

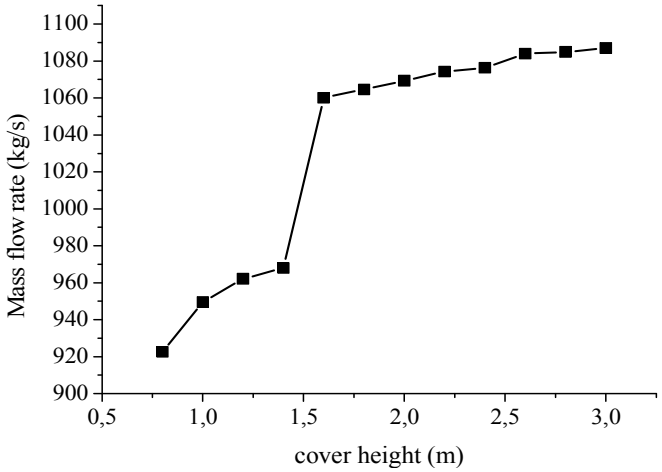


Fig. 11: Variation of mass flow rate with cover height

output quantities namely the exit velocity, the temperature increase within the system and the fluid and ground temperatures along the radial direction of the collector.

**Effect of collector radius:** Figure 9 displays the effect of collector radius on the Temperature rise (ΔT) and air velocity inside the collector under a solar radiation of 800 W/m$^2$. The numerical simulations are obtained for radius values of 40, 60, 80, 100, 120 and 140 m, respectively while maintaining the other parameters (tower size and solar radiation) constant. The figure indicates that ΔT is strongly affected by the collector radius variation. For example, for a radius of 140 m, ΔT is 21.64 K, which is 14.57 K higher than that corresponding to a collector radius of 40 m.

Figure 9 indicates also that air velocity increases linearly with the increase of the collector radius. For example, when the collector radius is 40 m, the velocity of the system is about 1.37 m/sec while it reaches 3.45 m/sec when the radius is 140 m. This can be attributed in part to the increase of the collected energy quantities. One can conclude that when the collector radius increases the driving buoyancy forces increase causing a higher velocity inside the chimney.

**Effect of collector entrance height:** The effects of the cover height, h (Fig. 2) on the exit velocity and temperature increase as well as on the mass flow rate are given in Fig. 10 and 11 respectively. It is seen that air velocity through the collector decreases as the collector height (varied from 0.8 to 3 m) increases causing a reduction in the heat transfer to the flowing air across the collector. The temperature rise decreases significantly with the increase of collector height. On the other hand, the cover height at the entrance must be as low as possible to prevent side winds from entering the chimney, thus removing the heated air in the cover.

Figure 11 shows that the increase in cover height increases the air mass flow rate entering the chimney. One can note that the mass flow rate behavior has two parts. In the first part corresponding to small values of h, the mass flow rate has a linear distribution with h with a relatively high slope: the cover height has strong effect on the mass flow rate. In the second part which starts after a critical value of the collector entrance height h (of about 1.4 m), the air flow rate increases slightly and remains almost constant when the height exceeds 2 m. From above analysis it can be said that there is a limit on the collector entrance height, above which no obvious profit for air flow rate can be attained. This is mainly due to the excessive heat losses occurred in the collector.

**Effect of chimney height:** The calculated mass flow rate in the solar chimney power plant is presented in Fig. 12 for different chimney height values. Several simulations were conducted based on the Spanish prototype configuration. The main dimensions of the prototype remain unchanged except for the chimney height which varies from 40 to 300 m. The study shows that an increase in height of the tower leads to an increase in mass flow rate inside the system. This increase is important mainly for low h values.

The influence of the tower height on the chimney inlet velocity and collector temperature increase is shown in Fig. 13. The solar radiation is fixed at 800 W/m$^2$. The increases of tower height results in higher exit velocity. This may be attributed to the increase of the solar energy surface area collection. However, such increase in the tower height is accompanied by a lower air temperature variation at the collector. The numerical results revealed that the chimney height is one of the most important geometric dimensions for solar chimney design. The higher the chimney height, the greater the driving force and thus the buoyancy differences.

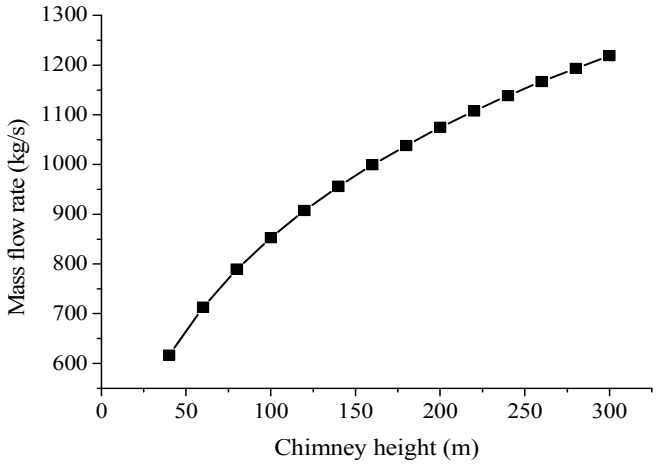


Fig. 12: Variation of mass flow rate with chimney height

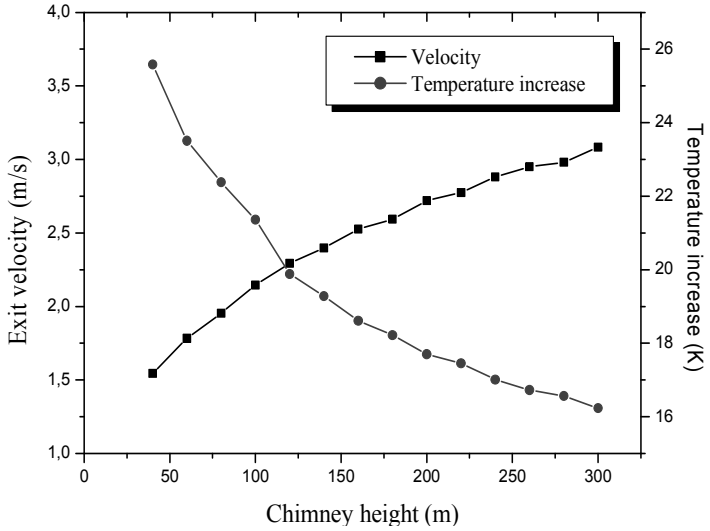


Fig. 13: Exit velocity and temperature rise versus chimney height (solar radiation = 800 W/m$^2$)

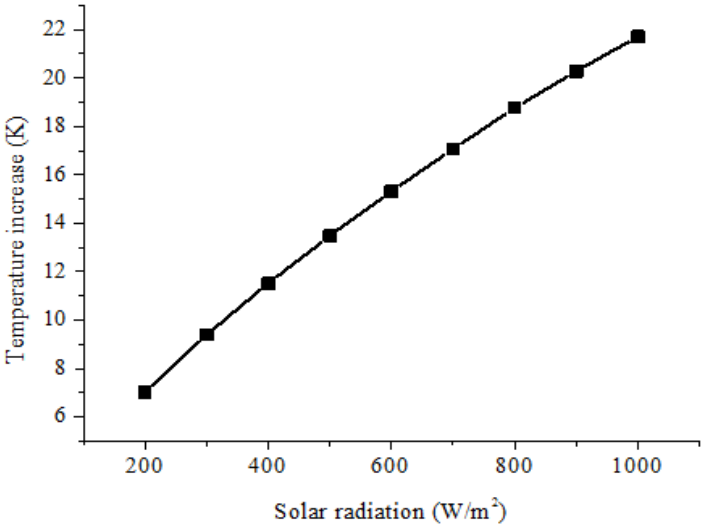


Fig. 14: Temperature rise versus solar radiation

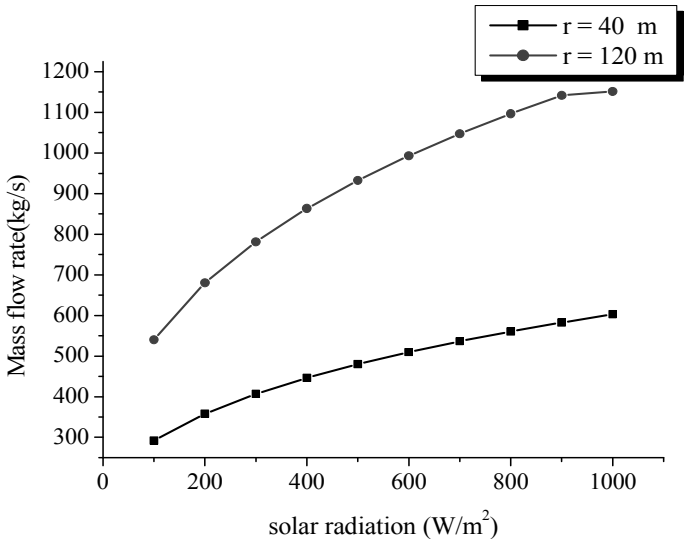


Fig. 15: Mass flow rate versus solar radiation

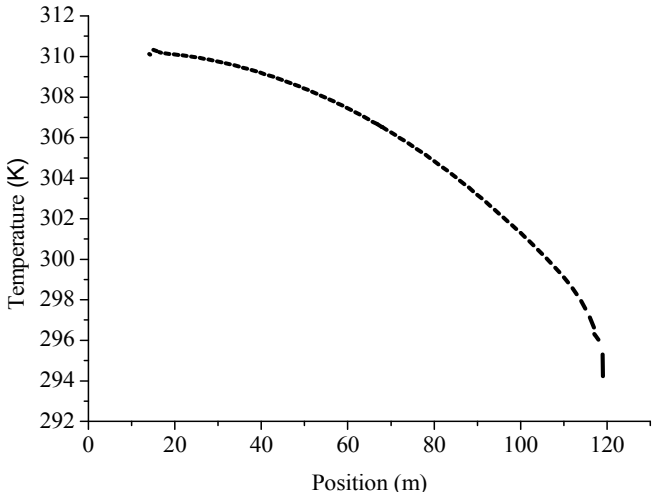


Fig. 16: Air temperature distribution across the collector

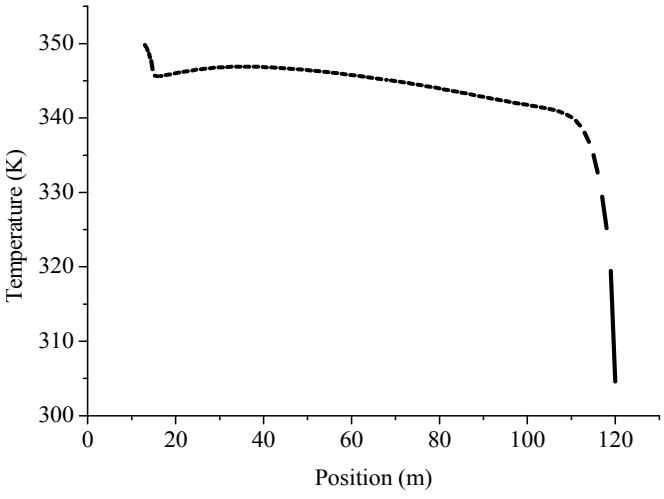


Fig. 17: Ground temperature distribution

**Effect of solar radiation:** Figure 14 displays the variation of airflow temperature difference inside the collector with the solar radiation. The solar radiation intensity varies between 200 and 1000 W/m$^2$. As it can be seen in Fig. 14, the air temperature change rises remarkably with the increase in the solar radiation: it increases from 7.01 to 21.7 K, as solar radiation rises from 200 to 1000 W/m$^2$. This is due to the fact that the increase in solar radiation causes the improvement of the heat quantity acquired by the flowing air through the collector.

Figure 15 depicts the mass flow rate as function of the solar radiation, for two different values of the collector radius. It is clear from Fig. 15 that the case of a radius of 120 m offers higher mass flow rate than that of a radius of 40 m. This behavior is expected since as the collector area increases more heat is absorbed causing the air temperature to rise while air density to drop. As density decreases, the driving pumping buoyancy effect increases and more air will flow through the chimney. For example, at a solar radiation level of 800 W/m$^2$, the air flow rate through a solar chimney with a collector radius of 120 m is in average about 32.3% higher than air flow rate through a chimney coupled to a collector of 40 m in radius.

Figure 16 and 17 shows the distribution of the fluid and ground temperature respectively along the radial direction of the collector for a given solar radiation of 800 W/m$^2$. From Fig. 16, it can be seen that the air entering the collector at a temperature of 293 K, is heated when it moves through the collector. The air temperature increases gradually along the collector by decreasing the radius: it increases from the periphery to the center of the solar chimney. This is due to the heat exchanges between the ground and the airflow.

Figure 17 indicates that the ground temperature increases along the radial direction of the collector. This Figure demonstrates also that ground temperature is higher than air flow temperature. Near the collector outlet, the temperature at the surface of the ground shows a slight drop then a sudden increase. According to Pasthor *et al*. (2004) and Hedderwick (2000), this is attributed to the high heat transfer coefficients present near the collector center resulting from the higher collector air velocities in this area.

## CONCLUSION

In this study, a numerical analysis on the performance of a solar chimney power plant using Three-Dimensional (3D) steady state Navier-Stokes and energy equations in cylindrical coordinate system was presented. The fluid flow inside the chimney is assumed to be turbulent and simulated with the k-ε turbulent model, using FLUENT software. Numerical simulations were performed using the Spanish prototype characteristics.

Reasonable agreements between numerical predictions and experimental measurements of temperature difference and outlet velocity in the collector were reported. The numerical model was also validated using previous numerical results.

Besides, a mathematical model based on energy and mass balances within the collector was established. The effect of kinetic energy contribution has been studied using this model and the Schlaich theoretical model proposed in the literature. It is found that the kinetic energy has a significant effect on the air velocity at the collector exit. Therefore, its contribution cannot be neglected.

A parametric study is also performed using the developed numerical model. The effects of the collector radius, collector height and the chimney height on the air mass flow rate and the temperature difference within the collector have been analyzed systematically. It is found that the solar chimney performance depends strongly on its geometric dimensions. For instance, the air mass flow rate rises significantly with the increase of the plant cover height in particular when the latter has small values.

## NOMENCLATURE

$A$ : Area (m$^2$)
$Ac$ : Cross sectional area of solar chimney (m$^2$)
$Acoll$ : Solar collector area (m$^2$)
$c_p$ : Specific heat capacity (J/kg/K)
D : Diameter of the collector (m)
$g$ : Gravity acceleration (msec$^{-2}$)
$G$ : Solar irradiance (W/m$^2$)
$H$ : Chimney height (m)
$h$ : Distance from the ground to the cover (m)
$hconv$ : Heat-transfer coefficient (W/m$^2$)
$\dot{m}$ : Mass flow rate (kg/sec)
$p$ : Pressure (Pa)
$q$ : Solar radiation (W/m$^2$)
$R$ : Collector radius (m)
$r$ : Radial coordinate (m)
$rc$ : Radius of the chimney (m)
$T$ : Temperature (K)
$u$ : Velocity in the radial direction (msec$^{-1}$)
v : Velocity in the axial direction (msec$^{-1}$)
V1 : Inlet air velocity of the solar collector (m/sec)
V2 : Outlet air velocity of the collector (m/sec)
$\dot{Q}$ : Heat gain of the air in the collector (W)
z : Axial coordinate (m)

**Greek symbols:**

$\beta$ : Volumetric coefficient of expansion (k$^{-1}$)
$\lambda$ : Thermal conductivity (W/m/k)
$\varepsilon$ : Emissivity
$\rho$ : Density (kg/m$^3$)
$\tau_\alpha$ : Transmittance-absorbtance product
$a$ : Ambient
$c$ : Cover
$coll$ : Collector

*ch* : Chimney
*1* : Inlet
*2* : Outlet
Δp : Pressure difference (Pa)
ΔT : Temperature increase between outlet and inlet of the collector (K)
Φp : Heat losses by convection (W/m)

## ACKNOWLEDGMENT

The third author (Dr. J. Orfi) extends his appreciation to the Deanship of Scientific Research at King Saud University (Research group project No: RGP-VPP-091).

## REFERENCES

Bernardes, M.A.d.S., R. Molina Valle and M.F.B. Cortez, 1999. Numerical analysis of natural laminar convection in a radial solar heater. Int. J. Therm. Sci., 38(1): 42-50.

Chergui, T., S. Larbi and A. Bouhdjar, 2010. Thermo-hydrodynamic aspect analysis of flows in solar chimney power plants: A case study. Renew. Sust. Energ. Rev., 14(5): 1410-1418.

Dai, Y., H. Huang and R. Wang, 2003. Case study of solar chimney power plants in Northwestern regions of China. Renew. Energ., 28(8): 1295-1304.

Fluent Inc., 2005. Fluent 6.3 User Guide. Fluent Inc., Lebanon, New Hampshire.

Haaf, W., 1984. Solar chimneys-part II: Preliminary test results from the Manzanares pilot plant. Int. J. Sol. Energy, 2: 141-161.

Haaf, W., K. Friedrich, G. Mayr and J. Schlaich, 1983. Solar chimneys part I: Principle and construction of the pilot plant in Manzanares. Int. J. Sol. Energy, 2: 3-20.

Hedderwick, R.A., 2000. Performance evaluation of a solar chimney power plant. M.Sc. Thesis, University Stellenbosch, pp: 128.

Huang, H.L., H. Zhang, Y. Huang and F. Lu, 2007. Simulation calculation on solar chimney power plant system. In: Cen, K., Y. Chi and F. Wang (Eds.), Challenges of Power Engineering and Environment. Springer, Berlin, Heidelberg, pp: 1158-1161.

Lorente, S., A. Koonsrisuk and A. Bejan, 2010. Constructal distribution of solar chimney power plants: Few large and many small. Int. J. Green Energy, 7: 577-592.

Ming, T., W. Liu and G. Xu, 2006. Analytical and numerical investigation of the solar chimney power plant systems. Int. J. Energ. Res., 30(11): 861-873.

Ming, T., W. Liu and Y. Pan, 2008b. Numerical analysis of the solar chimney power plant with energy storage layer. In: Goswami, D.Y. and Y. Zhao (Eds.), Proceeding of the ISES World Congress. Springer, Berlin, Heidelberg, 1/5: 1800-1805.

Ming, T.Z., Y. Zheng, C. Liu, W. Liu and Y. Pan, 2010. Simple analysis on thermal performance of solar chimney power generation systems. J. Energy Inst., 83(1): 6-11.

Ming, T., W. Liu, G. Xu, Y. Xiong, X. Guan and Y. Pan, 2008a. Numerical simulation of the solar chimney power plant systems coupled with turbine. Renew. Energ., 33(5): 897-905.

Patankar, S.V., 1980. Numerical Heat Transfer and Fluid Flow. Taylor and Francis, New York.

Pastohr, H., O. Kornadt and K. Gürlebeck, 2004. Numerical and analytical calculations of the temperature and flow field in the upwind power plant. Int. J. Energ. Res., 28(6): 495-510.

Pasumarthi, N. and S.A. Sherif, 1998a. Experimental and theoretical performance of a demonstration solar chimney model-Part I: Mathematical model development. Int. J. Energ. Res., 22(3): 277-288.

Pasumarthi, N. and S.A. Sherif, 1998b. Experimental and theoretical performance of a demonstration solar chimney model-Part II: Experimental and theoretical results and economic analysis. Int. J. Energ. Res., 22(5): 443-461.

Sangi, R., M. Amidpour and B. Hosseinizadeh, 2011. Modeling and numerical simulation of solarchimney power plants. Sol. Energy, 85(5): 829-838.

Schlaich, J., 1995. The Solar Chimney: Electricity from the Sun. Axel Menges Edn., Bergermann and Partner, Stuttgart.

Schlaich, J., R. Bergermann, W. Schiel and G. Weinrebe, 2005. Design of commercial solar updraft tower systems-utilization of solar induced convective flows for power generation. J. Sol. Energ-T. ASME, 127(1): 117-124.

Versteeg, H.K. and W. Malalasekera, 2007. An Introduction to Computational Fluid Dynamics: The Finite Volume Method. 1st Edn., Pearson Education Ltd.

Xu, G., T. Ming, Y. Pan, F. Meng and C. Zhou, 2011. Numerical analysis on the performance of solar chimney power plant system. Energ. Convers. Manage., 52(2): 876-883.

Zheng, Y., T.Z. Ming, Z. Zhou, X.F. Yu, H.Y. Wang, Y. Pan and W. Liu, 2010. Unsteady numerical simulation of solar chimney power plant system with energy storage layer. J. Energy Inst., 83(2): 86-92.